

# Construction of a High-Resolution Muon Drift Tube Prototype Chamber for LHC Upgrades

Bernhard Bittner<sup>†</sup>, Jörg Dubbert<sup>†</sup>, Matthias Kilgenstein<sup>†</sup>, Oliver Kortner<sup>†</sup>, Sandra Kortner<sup>†</sup>, Hubert Kroha<sup>†</sup>, Jörg von Loeben<sup>†</sup>, Robert Richter<sup>†</sup>, Philipp Schwegler<sup>†</sup>

**Abstract**—The proposed upgrade of the Large Hadron Collider at CERN to luminosities above  $1 \times 10^{34} \text{ cm}^{-2}\text{s}^{-1}$  necessitates the replacement of a large number of tracking chambers of the muon spectrometer of the ATLAS experiment to avoid deterioration of the muon identification and the momentum measurement at high background rates. Based on the standard ATLAS Monitored Drift Tube chambers ( $2 \times 3$  or  $4$  tube layers, drift tube diameter 30 mm), a new design with 15 mm diameter tubes and matching services has been developed, offering an increased rate capability and better pattern recognition and redundancy due to the higher cell density. A full-sized prototype chamber consisting of 1152 tubes arranged in  $2 \times 8$  tube layers and covering an area of  $1 \text{ m}^2$  has been built to validate the assembly procedures and to test its performance.

**Index Terms**—Muon chambers, drift tubes, high rates, LHC

## I. INTRODUCTION

THE muon detectors of the experiments at the Large Hadron Collider (LHC) have to provide a reliable muon identification and a precise momentum measurement in the presence of unprecedented high background radiation.

In the muon spectrometer of the ATLAS experiment [1] Monitored Drift Tube (MDT) chambers are used as precision tracking detectors. They consist of two triple or quadruple layers of aluminum drift tubes—mounted on an intermediate lightweight support frame—with an outer diameter of 30 mm, a wall thickness of 0.4 mm, and a single centered anode wire of 50  $\mu\text{m}$  diameter. Operated with an Ar/CO<sub>2</sub> (93/7) gas mixture at a pressure of 3 bar absolute and a potential of 3080 V applied between the tube wall and the anode wire, the individual drift tubes reach an average spatial resolution of 80  $\mu\text{m}$  and have a maximum drift time of 700 ns at low background rates; in conjunction with the wire positioning accuracy of better than 20  $\mu\text{m}$ , the MDT chambers reach a spatial resolution of 35  $\mu\text{m}$ . The drift tube chamber design offers several advantages: modularity in the construction and mechanical robustness, operational independence of each tube leading to negligible inefficiencies in case of failures, and the independence of the spatial resolution from the angle of incidence of the particle track. The ATLAS MDT chambers were designed to cope with counting rates up to 300 KHz per tube, corresponding to an occupancy of about 20%. With the planned luminosity upgrade of the LHC beyond its design luminosity of  $1 \times 10^{34} \text{ cm}^{-2}\text{s}^{-1}$ , leading to an increase in the

background, of the chambers will exceed these counting rates in the forward regions of the spectrometer.

The rate capability of drift tubes can be improved by reducing the tube diameter. We report on the construction of a full-sized prototype chamber with 15 mm diameter tubes suitable to replace the ATLAS MDT chambers in the forward region of the experiment.

## II. DRIFT TUBE PERFORMANCE AT HIGH RATES

At high counting rates, the detection efficiency of the drift tubes of the ATLAS MDT chambers suffers from the increased occupancy [2] and the spatial resolution is degraded by the high space charge within the tubes [3], [4]. Both effects can be suppressed by reducing the tube diameter while keeping the other operating parameters, in particular the gas mixture, the pressure and the gas gain, unchanged.

A decrease of the drift tube diameter from 30 mm to 15 mm and of the operating voltage from 3080 V to 2730 V leads to a reduction of the maximum drift time by a factor of 3.5 from about 700 ns to 200 ns [5], see fig. 1. In addition, the background counting rate, dominated by the conversion of the neutron and gamma background radiation in the tube walls, decreases proportional to the tube diameter, i.e. by a factor of two per unit tube length. Both effects together lead to a reduction of the occupancy by about a factor of 7.

The space charge of the ion clouds created in the avalanches and drifting towards the tube wall lowers the effective potential near the anode wire, leading to a reduction of the gas gain. The resulting loss in signal height and, therefore, spatial resolution grows with the inner tube diameter  $d$  proportional to  $d \cdot \ln(d/d_{\text{wire}})$  [6] where  $d_{\text{wire}}$  is the wire diameter. Therefore, the signal height reduction due to space charge is 10 times smaller in 15 mm compared to 30 mm diameter tubes. Fluctuations of the space charge and, consequently, of the electric field in the tube lead to variations of the drift velocity in nonlinear drift gases like Ar:CO<sub>2</sub> (93:7) causing a deterioration of the spatial resolution which increases rapidly with the drift distance above a value of about 7.5 mm [3], [4], cp. fig. 2. In addition, the space-to-drift time relationship for the Ar:CO<sub>2</sub> (93:7) drift gas is more linear at drift distances below 7.5 mm (see fig. 1), reducing the sensitivity of the position measurement to environmental parameters such as gas composition and density, magnetic field and, in particular, irradiation rate.

With the smaller drift tube diameter the cell density can be increased by a factor of 4 in the same detector volume, allowing for additional improvement of the detection efficiency and spatial resolution of the chamber.

<sup>†</sup> Max-Planck-Institut für Physik (Werner-Heisenberg-Institut), Föhringer Ring 6, D-80805 München, Germany  
Corresponding author: J. Dubbert, joerg.dubbert@mppmu.mpg.de

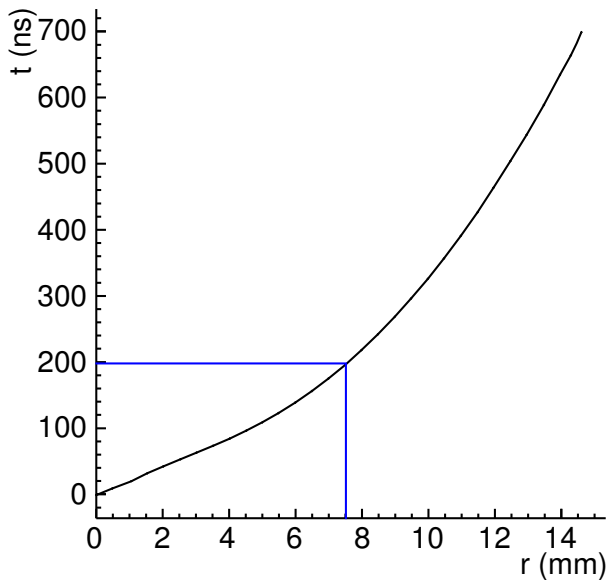


Fig. 1. Simulated space-to-drift time relationship of 30 mm diameter drift tubes. If the tube diameter is reduced to 15 mm, the maximum drift time is reduced from 700 ns to about 200 ns (blue lines).

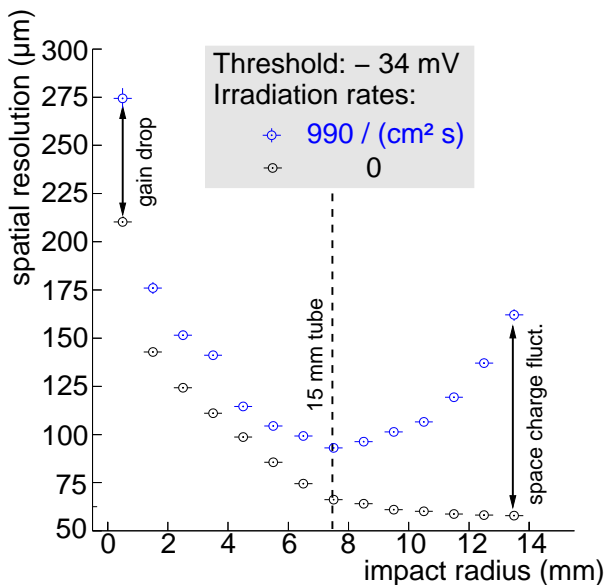


Fig. 2. Resolution of 30 mm diameter drift tubes for different photon irradiation rates, measured at the Gamma Irradiation Facility at CERN with an  $^{137}\text{Cs}$  source [2]. The degradation of the resolution by space charge fluctuations is reduced for drift drift distances below 7.5 mm, corresponding to 15 mm tubes (dashed line). See text for a discussion of the gain drop effect.

Since the drift-tube spatial resolution at low background rates improves with the drift distance, the average single tube resolution deteriorates from  $80\ \mu\text{m}$  for 30 mm diameter tubes [2], [4] to about  $110\ \mu\text{m}$  for 15 mm diameter tubes. For 30 mm diameter drift tubes, the resolution has been measured to deteriorate approximately linearly with the counting rate to about  $120\ \mu\text{m}$  at  $500\ \text{Hz}/\text{cm}^2$  [2], [4]. For 15 mm diameter tubes, the rate dependence of the resolution, dominated by the gain drop effect, is expected to be about 10 times smaller.

### III. DESIGN OF THE 15 MM DRIFT TUBES AND THE PROTOTYPE CHAMBER

Figure 3 shows an exploded view of a 15 mm diameter drift tube. The central part of the design is the end-plug which, in addition to electrically insulating the anode wire and providing the necessary inlets and outlets for the gas flow, transfers the internal wire position to an external reference surface available during the chamber assembly: the injection molded PBT plastic piece contains a precision brass insert which holds the wire locator (twister) which fixes the wire position to within a few micrometers. An aluminum ring adds structural support to the end-plug body. Each end-plug is crimped to the tube and seal the gas volume with an O-ring. The wire ends are crimped to two copper ferrules which are held in place longitudinally by the brass insert and keep the wire tensioned. A connector of the modular gas distribution system is fixed by the signal cap which also facilitates the electrical contact to the anode wire. Grounding pins are inserted between the tubes providing the necessary contact to the tube walls and the end-plug by the threading and the contact disk.

The prototype chamber (see fig. 4) was designed to fit into the forward region of the ATLAS muon spectrometer in which the detectors are arranged in a disk perpendicular to the beam direction. Therefore, the chamber has a trapezoidal shape created by 3 different drift tube lengths of 560 mm, 760 mm, and 960 mm. The available space allows  $2 \times 8$  tube layers with 72 tubes each, giving a total of 1152 tubes, about three times more than largest ATLAS MDT chambers in use.

### IV. DRIFT TUBE PRODUCTION AND QUALITY ASSURANCE

The production of a drift tube proceeds in the following steps:

- 1) Assembly of the end-plug by inserting the twister and stopper.
- 2) Feed-through of the wire through the tube with a clean air flow.
- 3) Threading of the wire through the end-plugs.
- 4) Crimping a ferrule on one wire end to fix it to the end-plug.
- 5) Crimping of both end-plugs to the tube.
- 6) Applying a tension of 350 g to the free wire end using a spring balance.
- 7) Crimping of a ferrule to the second wire end to fix it.

The aluminum tubes used are standard tubes available from industry with tolerances of  $\pm 0.1\ \text{mm}$  on diameter, roundness and concentricity and of  $\pm 0.5\ \text{mm}$  on straightness.

The assembly is carried out in a clean room to avoid contamination of the wire and inner tube surface. For the tube production of the prototype chamber all steps were carried out manually. The daily drift tube production rate is shown in fig. 5. A total of 1204 drift tubes were produced in a time frame of four weeks with a manpower of 2 people. The average production rate amounted to about 80 tubes per working day with a peak value of 160 tubes per working day. A semi-automated, computer controlled, machine for wire-tensioning (including pre-tensioning) and tube crimping has been set up for a future series production.

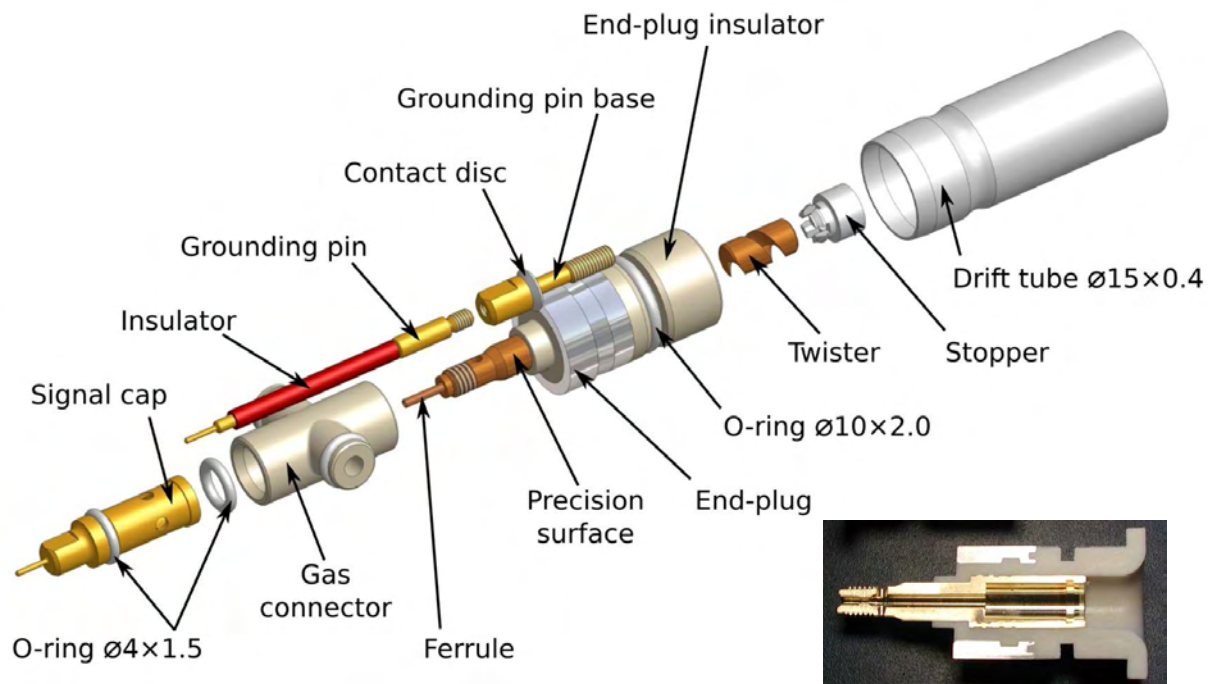


Fig. 3. Exploded view of a 15 mm diameter drift tube. The units of the dimensions are mm. The lower right corner shows a photograph of a cut, yet unmachined, end-plug

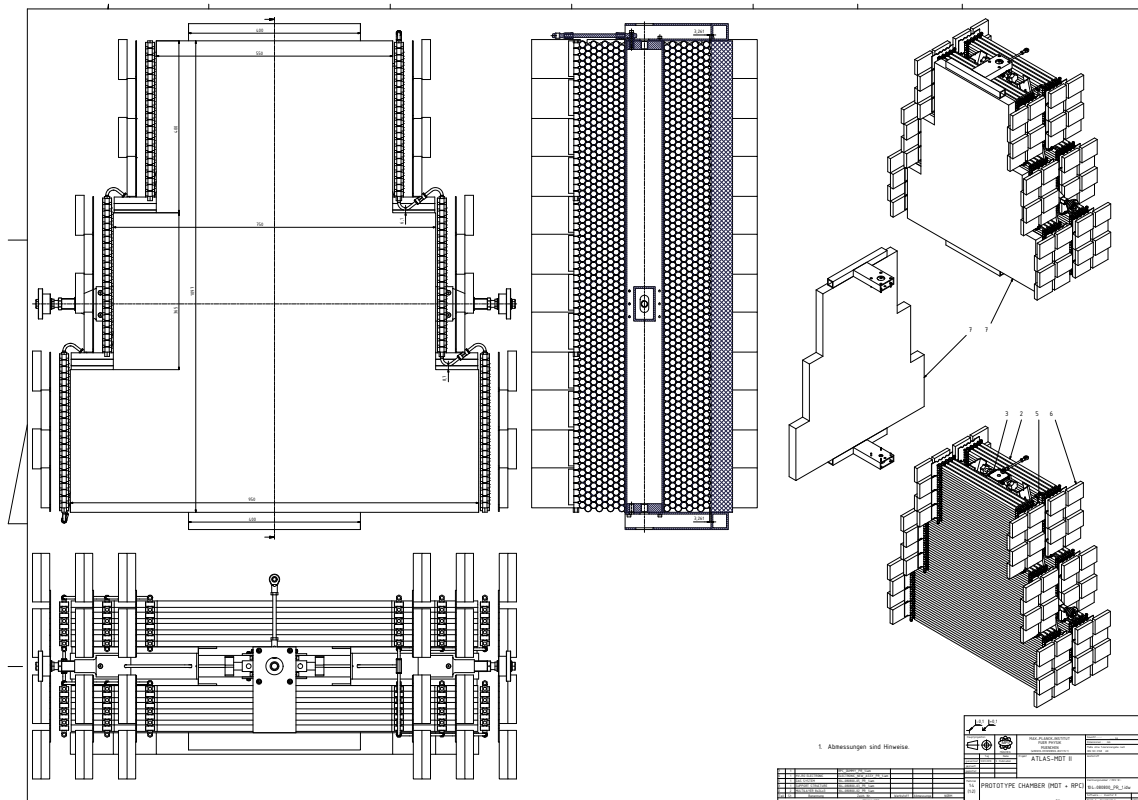


Fig. 4. Technical drawing of the prototype chamber. The front-end electronics currently extend beyond the tube envelope; this is due to the re-use of the active ATLAS read-out electronic cards, designed for chambers with 30 mm diameter drift tubes and the need to accommodate a four times higher channel density. On the upper right side, the drawing also shows how an optional trigger chamber can be mounted on the drift tube chamber.

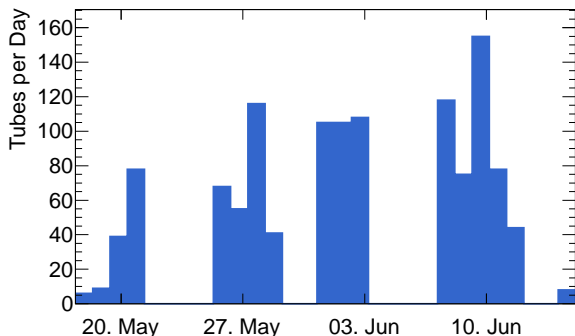


Fig. 5. Daily drift tube production rate. The average production rate was 80 drift tubes per day assembled by 2 people.

QA Test	Tested Tubes	Passed	Failure Rate (%)
Wire Tension	1204	1129	6.3 <sup>1</sup>
Leak Test	1171	1164	0.6
HV	1164	1159	0.4
<b>Total</b>	<b>1208</b>	<b>1116</b>	<b>7.7</b>

TABLE I

FAILURE RATES OF PRODUCED DRIFT TUBES AT THE QUALITY ASSURANCE (QA) TESTS. TUBES WHICH HAD FAILED IN ONE FIELD WERE NOT FURTHER TESTED.

All drift tubes were tested for their wire tension, high voltage stability and gas tightness immediately after production. The applied criteria and limits were chosen to conform with the stringent requirements used during the production of the ATLAS MDT chambers:

- wire tension of  $(350 \pm 15)$  g
- gas leak rate below  $10^{-5}$  mbarL/s
- dark current below 5 nA at an over-voltage of 3015 V (corresponding to a 32-fold increase of the gas gain compared to the normal operating voltage of 2730 V)

The wire tension of each tube was measured with a CAEN SY502 wire-stretch meter. The gas leak rate was determined with a Leybold UL 500 helium leak detector, applying helium to the outside of the tube ends and measuring its inflow into the evacuated drift tube. Finally the high voltage test was carried out in parallel for 5 tubes using an Iseg SHQ 224 power supply and its internal current measurement with nA resolution. In case of failures the tubes were retested individually.

Table I summarizes the number of tested tubes and the failure rates of the tests. In total 1120 tubes have passed all tests while 1152 tubes are necessary for constructing the prototype chamber. Hence, 32 tubes with a wire tension slightly outside the tolerance range had to be used. The high failure rate of the wire tension test occurred only at the beginning of the production and was later eliminated by a recalibration of the tensioning setup. Figure 6 shows the measured wire tension of all tubes.

## V. CHAMBER ASSEMBLY

The chamber assembly uses special precision jigs mounted on a granite table. A comb-like structure into which the tubes

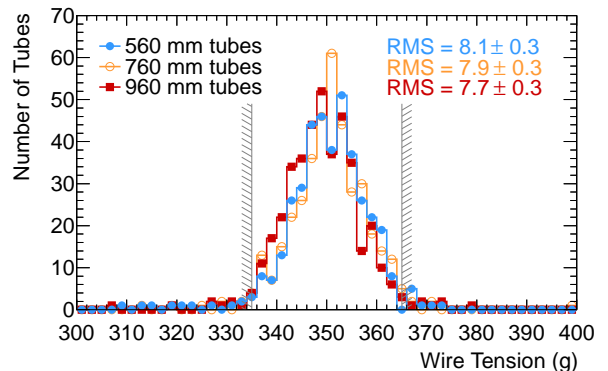


Fig. 6. Measured wire tension of all tubes. The allowed limit is designed by the hatched lines. The different colors denote the different tube lengths.

are inserted at the precision surfaces of the their end-plugs ensures the high mechanical precision and the knowledge of the wire positions to better than  $20 \mu\text{m}^1$ . To allow for the trapezoidal chamber shape, each tube length each jig consists of 3 separate parts. A tube layer is inserted into the jigs, spacers of 0.1 mm thickness are fixed to all tubes to constrain the distance to the next tube layer at several points along each tube, and glue is applied to the tube surfaces facing the next layer. The jigs for the next tube layer are then mounted. This procedure is repeated until all (8 in the case of the prototype chamber) tube layers of a multilayer are assembled, resulting in the assembly of several tube layers in a single day. After the glue is cured, the spacer frame which separates the two multilayers of the chambers is glued on the first multilayer. The half finished chamber is lifted off the assembly table after curing of the glue and the second multilayer is assembled. Finally, the inverted first multilayer with the spacer frame is glued to the second multilayer. The assembly stages are illustrated in Figure 7. As soon as the chamber is finished, the bases of the ground pins are be screwed into the free space between 3 adjacent tubes. This procedure turned out to be very time-consuming and the bases were redesigned such that in the future they can already be inserted in the gluing stage and the electrical connection is no longer established by a screw thread but a spring.

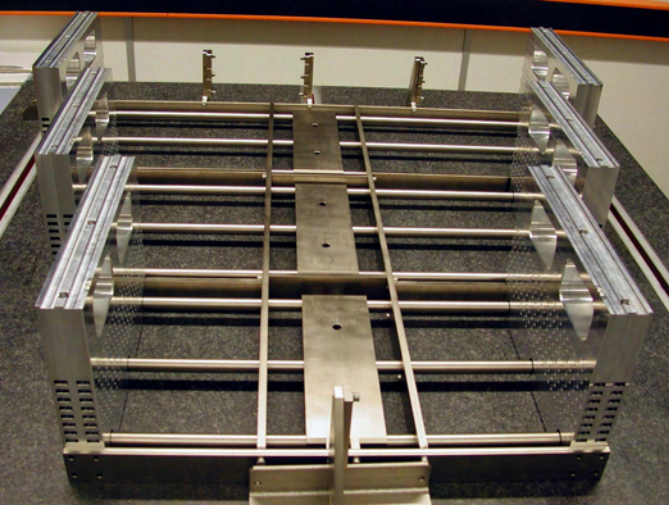
## VI. ON-CHAMBER SERVICES

The high channel density of a chamber with 15 mm diameter drift tubes compared to the standard ATLAS MDT chambers necessitated the development of a new gas distribution system and new passive front-end electronic cards for the high voltage distribution and the signal read-out.

### A. Gas Distribution System

The modular gas system distributes the gas flow in parallel to all drift tubes. On each segment of the chamber containing

<sup>1</sup>The achievable accuracy of the wire position knowledge was confirmed on a  $8 \times 12$  tube test bundle in a cosmic ray test stand at Munich University [7]. The measurement of all wire positions of this prototype chamber in the same facility is scheduled for February 2011.



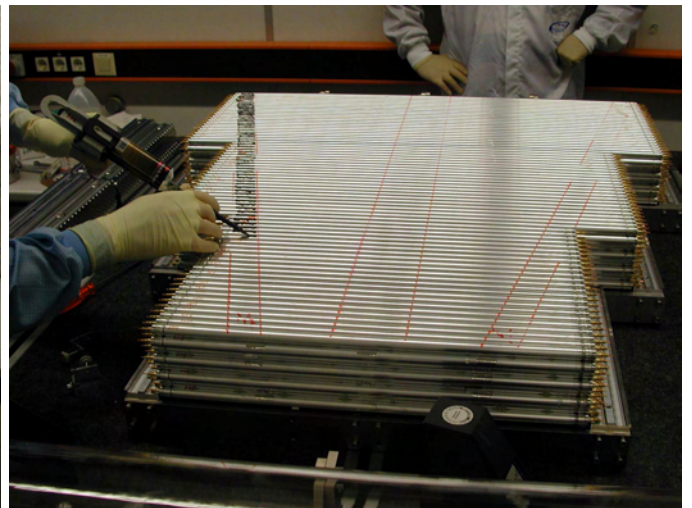
(a) The precision jigs.



(b) Lay-up of the first tube layer.



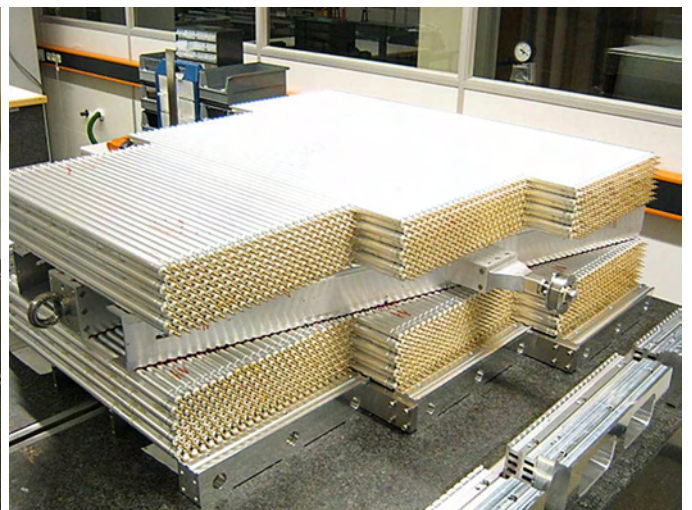
(c) Gluing of the second tube layer onto the first one.



(d) Applying the glue for the spacer.



(e) The spacer glued onto the first multilayer.



(f) Both multilayers with the spacer glued between them.

Fig. 7. Stages of the chamber assembly. The eight tube layers comprising a multilayer can be glued in a single day.

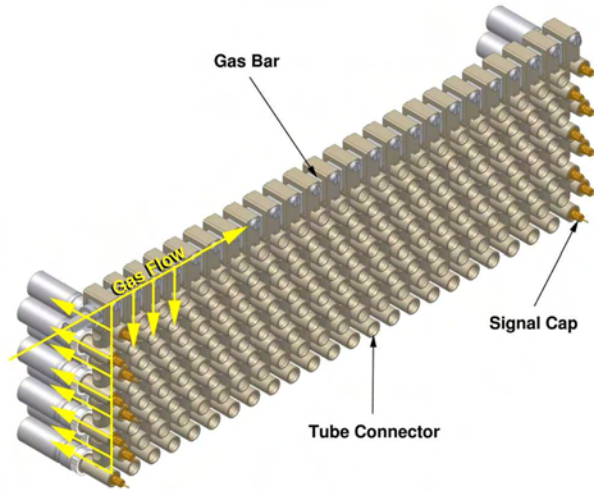


Fig. 8. Drawing of the on-chamber gas distribution system. The yellow arrows indicate the gas flow in the system.

tubes of the same length, the gas enters a so-called gas bar on top of the outermost tube layer. The gas bars themselves are interconnected with 6 mm stainless steel pipes of 1 mm wall thickness. The gas is then distributed to chains of 8 connectors, each of which supplies a tube in one of the eight tube layers. The connectors are held in place by and encompasses the signal caps while leaving space for the grounding pins to pass through between them. Small holes with high impedance in the signal caps and in the brass insert of the end-plugs allow a portion gas to enter each tube, while the main gas flow is further distributed. On the other tube sides the same system is used to collect the output flow. The inlet and outlet connections of each multilayer are situated diagonally across on different sides of the multilayer to maximize their relative impedance and allow equal gas flow through all drift tubes. Figure 8 shows a drawing of the gas distribution system.

### B. Passive Front-End Electronic Cards

The drift tubes are supplied on one tube end with high voltage and read-out on the other end.

On the high voltage side, daisy-chained front-end cards distribute the voltage to  $4 \times 6$  tubes each. Each tube is terminated to avoid signal reflection and supplied via a low pass filter (the of this filter resistor also limits the maximum current in case of a short circuit caused e.g. by a broken anode wire), cp. fig. 9. The small space available did not allow to mount all components on a single circuit board. Instead, the termination resistor is housed in a small insulated barrel for each channel while the resistor and the capacitance are mounted on the circuit board on top. A second, stacked, circuit board contains the distribution network, see fig. 10.

On the read-out side, the drift tube signals are AC-coupled and the impedance is matched to the amplifier, cp. fig. 11. Again, due to space limitations and to ensure high voltage stability, a three-dimensional structure is used instead of a single circuit board: the decoupling capacitance is enclosed in the barrel while the protection and input resistors are mounted in SMD technology on the circuit board on top, see fig. 12. The

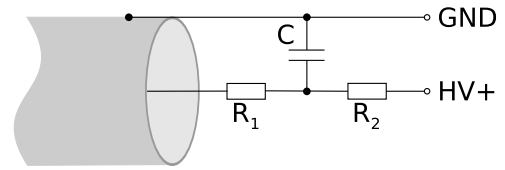


Fig. 9. Circuit diagram of the high voltage distribution,  $C = 100$  pF,  $R_1 = 330 \Omega$ ,  $R_2 = 1$  M $\Omega$

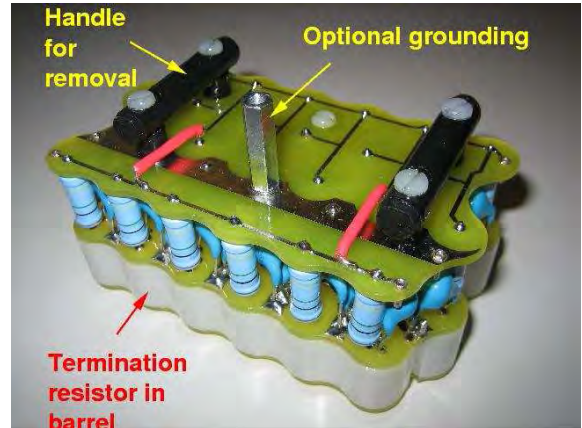


Fig. 10. Photograph of the high voltage distribution front-end card.

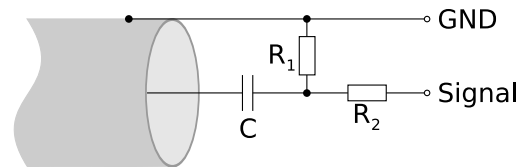


Fig. 11. Circuit diagram of the read-out coupling,  $C = 100$  pF,  $R_1 = 10$  k $\Omega$ ,  $R_2 = 10 \Omega$

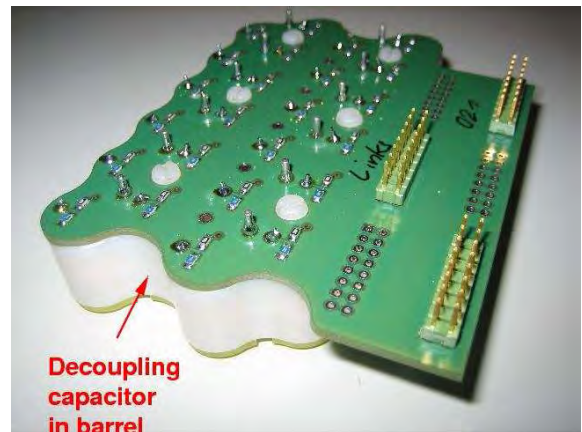


Fig. 12. Photograph of the passive read-out front-end card. An active front-end electronic card is plugged onto the pole connectors.

three pole connectors allow a standard ATLAS MDT active front-end card, containing amplifier, shaper, discriminators and a TDC for the drift time measurement of 24 channels, to be plugged onto this card.

## VII. CONCLUSION

The Max-Planck-Institut für Physik has built a prototype chamber consisting of 1152 tubes of 3 different lengths. More than 1200 drift tubes have been successfully produced and tested for wire tension, gas tightness and high voltage stability. The total failure rate of the drift tube production of 7.7% was dominated by a miscalibration of the wire tensioning setup at the beginning of the production; subsequently the failure rate was below 1%. The chamber assembly procedures have been validated and the time frame of 1 day for the gluing of 8 tube layers has been confirmed, resulting in a possible mass production rate of 1 chamber per 3 days. A new modular gas system and new passive front-end electronics cards for the high voltage distribution and read-out, fitting the high cell density, have been developed. The prototype chamber has been successfully operated over 5 weeks at muon and gamma irradiation test beams at CERN [8]. During the construction of this prototype several improvements to the chamber design and the assembly procedures have been identified and will be implemented in the future.

## ACKNOWLEDGMENT

The authors would like to thank the engineering department, the mechanical and the electronics workshops of the Max-Planck-Institut für Physik for their help in the realization of the prototype chamber and their support during its test.

## REFERENCES

- [1] The ATLAS collaboration, The ATLAS Experiment at the CERN LHC, JINST 3 S080003 (2008).
- [2] S. Horvat et al., Operation of the ATLAS Precision Muon Drift-Tube Chambers at High Background Rates and in Magnetic Fields, IEEE Trans. on Nucl. Science Instr., Vol. 53, No. 2 (2006) 562.
- [3] M. Aleksa et al., Rate Effects in High-Resolution Drift Chambers, Nucl. Instr. and Meth. A 446 (2000) 435.
- [4] M. Deile et al., Performance of the ATLAS Precision Muon Chambers under LHC Operating Conditions, Nucl. Instr. and Meth. A518 (2004) 65.
- [5] B. Bittner et al., Development of Muon Drift-Tube Detectors for High-Luminosity Upgrades of the Large Hadron Collider, Nucl. Instr. and Meth. A (2009), doi:10.1016/j.nima.2009.06.086.
- [6] W. Riegler, High Accuracy Wire Chambers, Nucl. Instr. and Meth. A494 (2002) 173.
- [7] O. Biebel et al., Test and calibration of large drift tube chambers with cosmic rays, IEEE Trans. on Nucl. Science Instr., Vol. 52 (2005) 2998.
- [8] J. v.Loeben et al., Performance of Fast High-Resolution Muon Drift Tube Chambers for LHC Upgrades, proceedings of the 2010 IEEE Nuclear Science Symposium, Knoxville, Tennessee, United States of America, 1-5 November 2010, Nuclear Science Symposium Conference Record 2010, IEEE, 2010.